Biocompatibility and bioactivity behaviour of coelectrospun silk fibroin-hydroxyapatite nanofibres using formic acid

Sara Zadegan[1], *Bahman Vahidi*[1] ✉, *Jhamak Nourmohammadi*[1] ✉, *Nooshin Haghighipour*[2]

[1]*Division of Biomedical Engineering, Department of Life Science Engineering, Faculty of New Sciences and Technologies, University of Tehran, Tehran, Iran*
[2]*National Cell Bank of Iran, Pasteur Institute of Iran, Tehran, Iran*
✉ *E-mail: bahman.vahidi@ut.ac.ir; J_nourmohammadi@ut.ac.ir*

Published in Micro & Nano Letters; Received on 19th January 2018; Accepted on 2nd February 2018

Appending hydroxyapatite (HAp) to non-osteogenic silk fibroin (SF) scaffolds is an undeniable fact about the bone tissue engineering. The present research aimed to fabricate the uniform coelectrospun SF-HAp composites with 1, 3 and 5 wt% of nano-particles using acid solution to access fibres with favourable mechanical strength simultaneous with the enhanced bone cell compatibility. SEM images displayed that the average diameter of nanofibres increased from 90 ± 12 in SF nanofibres to 227 ± 13 in SF-5%HAp. Meanwhile, the elastic modulus and breaking strain were equal to 63.4 ± 1.08 MPa and 2.57 ± 0.04, respectively, for SF-3% HAp which was significantly higher than the SF fibres. Bioactivity property was evaluated after immersion in simulated body fluid by the SEM/EDS analysis. The results, which were confirmed by XRD and FTIR, asserted calcium phosphate deposition after 7 days rather than the SF mats. Finally, the MTT assay, Alkaline Phosphatase (ALP) activity, calcium deposition and cell adhesion approved that the SF-HAp nano-composite could raise the cell viability and significantly enhance osteogenic differentiation and mineralisation process by increasing osteoblast cell migration and adhesion to the surface of nanofibres. In brief, it can be concluded that the SF-HAp nanofibres can be considered as the superlative candidates for application in the bone tissue engineering.

1. Introduction: Silk fibroin (SF), which is extracted from a variety of silkworms, is one of the most famous, plentiful and inexpensive natural proteins which account for one of two major constructing proteins of silk [1, 2]. Desirable properties such as cytocompatibility, controllable biodegradability, superior mechanical strength and diversity in products confirm the SF as one of the useful biomaterials for cell scaffolds [3, 4]. Electrospinned SF nanofibre has become an excellent candidate for the bone tissue engineering due to its high surface for volume ratio with interconnected porosity, simple fabrication method and copied extra cellular matrix [5]. In spite of the above-mentioned advantages, the pure SF nanofibres are rarely applied alone as a scaffold for bone regeneration because of their non-osteogenic behaviour [6]. Different methods have been used to enhance effectiveness of SF protein. For instance, the modification of SF nanofibres by soaking in simulated body fluid (SBF) did not result in powerful bonding between Hap and nanofibres along with the lack of controlling particle size and formation [7]. In other papers, hydroxyapatite (HAp) nano-particles were appended to SF, but the nano-particle agglomeration was the main challenge due to entangling hydrophil HAp particles in hydrophob SF matrix [8, 9]. Some research groups used a mixture of an aqueous SF solution with Hap immediately before ejection to prevent nano-particle precipitation, but the sedimentation possibility increased by over 30-min electrospinning and bond formation between hydroxyl groups in hap and SF leading to difficult electrospinning [10]. In other attempt, Hap nanoparticles were modified with a silane coupling agent for uniform dispersion in SF aqueous solution before electrospinning leading to a partly improved tensile strength along with nano-particles aggregated by increasing their amounts and exhibiting no significant cytocompatibility [11]. Some researchers sought to prepare these nanofibres using formic acid (FA). For instance, degummed SF films were performed by fa/hap dissolution which led to the higher mechanical properties. In another study, the electrospun sf/hap scaffolds were built by FA as the solvent in which the nanoparticles partly improved mechanical properties, but the average diameter increased 95 nm in the pure SF to 582 nm in 30% of hap nano-composite [12, 13]. Even if both studies focused on the uniform dispersion of HA nano-particles, none of them described the bioactivity and cytocompatibility of electrospun sf/hap nanocomposites with FA.

In the present study, we aimed to coelectrospin the SF-HAp nanofibres with small amounts of nano-particles including 1, 3 and 5 wt% in order to improve tensile strength and not significantly affect the rheological behaviour of solution and the average diameter of nano-fibres. Meanwhile, the present study initially investigated effects of acid solution on biological and bioactivity properties of nano-fibres. The bioactivity property was assessed by immersion in SBF, and the biocompatibility, cell adhesion, ALP activity and Ca deposition were studied through the MG-63 cells.

2. Materials and methods

2.1. SF/HAp solution preparation and electrospinning: *Bombyx mori* SF was provided according to previous published procedures [14]. Electro-spinning solution was provided by dissolution of freeze-dried SF in FA in order to produce 13 wt% of SF solution. The HAp nanoparticles were added to SF solution with different mass ratios of HAp to SF (1, 3 and 5 wt%). Electrospinned system (Fanavaran Nano-Meghyas Company, Iran) parameters were set before exerting 20 kV voltage as follows: The needle tip to collector distance in addition to the flow rate of solution were fixed on 13 cm and 0.25 ml h^{-1}, respectively. Finally, the nanofibres were immersed in methanol for 10 min in order to significantly reduce the water dissolution rate of nanofibres by inducing β-sheets conformation [15].

2.2. SF/HAp nano-fibres characterisation: The morphology of these mats was shown by the SEM (AIS2300C, South Korea), and the fibre diameter was evaluated by obtaining the average SF/HAp nano-fibres using Image J analysis software. Tensile strength and Young's modulus of SF/HAp nanofibres were looked through a universal testing machine. Tests were performed using 0.2 N as an initial load at the speed of 5 mm min^{-1}. Nanofibre mats were

20 mm × 5 mm in dimension with a thickness of 10 μm ($n = 3$ per group).

All nanofibres were exposed to SBF in order to find out their bioactive potential. To stimulate the in vivo condition, the SF/HAp nanofibres were soaked in 1.0 SBF (2 m, pH = 7.4) and placed in a shaker incubator at 37°C for 7 days. Every other day, some of the SBFs were replaced with the new solution. Samples were finally prepared for SEM/EDS analysis. In addition, the calcium phosphate deposition structure was considered by XRD (X'Pert Pro MPD) by application of Cu Kα radiation (40 mA and 40 kV) and FTIR (Equimo55 Bruker, Germany) ranging from 400 to 4000 cm^{-1}.

2.3. Biological evaluation: Human osteoblast-like cells, MG-63 (Pasteur cell bank, Iran), were cultured in RPMI1640 (Gibco BRL, Rockville, MD) supplemented with 10% of foetal bovine serum (Gibco, Renfrewshire, Scotland), 1% penicillin/streptomycin (Sigma, St. Louis, MO) and then incubated at 37°C in 5% of CO_2 atmosphere. Before cell seeding, the SF/HAp nano-fibre mats ($n = 3$) of each group were sterilised by their immersion in ethanol 70% for 45 min, and they were then washed three times with PBS.

Cell viability was examined through the indirect 3-dimethylthiazol-2, 5-diphenyltetrazolium bromide (MTT, Sigma, USA) assay [16] for 3, 7 and 14 days. The control of this test includes the wells of SF nanofibres without HAp. The osteogenic differentiation was investigated using ALP kit protocol (PARS-AZMON, Tehran, Iran) by measuring the optical density with a spectrophotometer at 405 nm. Calcium mineral deposition was then measured by PARS-AZMON kit protocol after 3, 7 and 14 days.

Cell adhesion assay was performed to investigate the interaction between the osteoblast and the surface of nanofibres after 3 days. Nano-fibre mats were fixed through 4% (v/v) glutaraldehyde solution in PBS at room temperature for 20 min. The dried samples were finally coated by gold sputtering, and then beheld by the SEM.

3. Results and discussion

3.1. Morphology of SF-Hap nanofibres: SEM images of SF-HAp nanofibres are clearly displayed in Fig. 1 and all of mats lack any bead indicating that electrospinning parameters were favourable. The measurement results of SF-HAp nanofibres with Image J software are presented in Table 1, indicating that the average diameter of nanofibres was gradually increased by growing HAp nano-particles, and these values increased from 90 ± 12 nm in SF nanofibres to 227 ± 13 nm in SF-5%HAp.

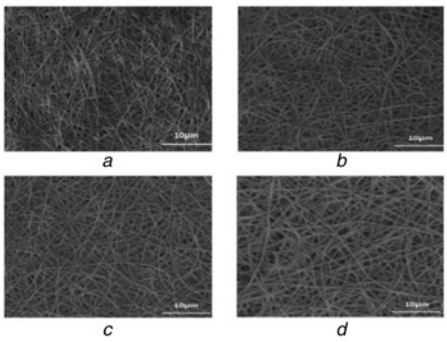

Fig. 1 *Electrospun fibres morphology with different HAp nano-particles contents*
a 0%
b 1%
c 3%
d 5%

Table 1 Average diameter of different SF-HAp nano fibres ($N = 100$)

Sample	Average nanofibre diameters, nm (± std dev)
SF-0%Hap	90 ± 12
SF-1%Hap	143 ± 15
SF-3%Hap	173 ± 7
SF-5%Hap	227 ± 13

Table 2 Mechanical properties of different SF-HAp nano fibres

Sample	Modulus, MPa	Extension at break, %
SF-0%Hap	38.05 ± 2.43	1.54 ± 0.05
SF-1%HAp	58.07 ± 1.57	1.75 ± 0.04
SF-3%Hap	63.4 ± 1.08	2.57 ± 0.04
SF-5%HAp	42.5 ± 2.35	1.62 ± 0.04

3.2. Mechanical strength of SF-HAp nanofibres: Mechanical properties of nanofibres are presented in Table 2. Results of tensile test indicated that the appropriate amount of HAp particles and their entanglement in SF fibres could lead to the fracture toughness increment. Moreover, the elastic modulus of SF nanofibres increased from 38.05 ± 2.43 MPa in SF mats to 58.07 ± 1.57, 63.4 ± 1.08 and 42.5 ± 2.35 MPa in 1, 3 and 5% of SF/Hap, respectively. Despite the fact that there is a suitable interaction between the ceramic particles and SF nano-fibres in 1 and 3% of HAp samples, SF-5% HAp samples have less mechanical properties. This may be due to the reduction of uniform distribution and increase in the possibility of agglomeration which diminishes the positive effect of HAp nanoparticles in polymer matrix by reducing the interconnection of fibres [17, 18].

3.3. Apatite formation on nano-fibres in SBF: The bioactivity property difference between electrospun composites was revealed by SEM/EDS analysis after 1, 4 and 7 days of immersion in SBF. No apatite deposition was seen on SF nanofibres until the end of day 7, and it reapproved the lack of osteoconductive property of SF, whereas the calcium phosphate deposition was beheld in SF/HAp nanofibres only after 24 h of immersion in SBF and increased by increasing the immersion time or HAp nano particles (Fig. 2). There were clear pores between nanofibres in SF-1% HAp after day 7, but the surface was entirely concealed in SF/3% HAp only at the end of day 4, and a thick and multilayer precipitation was formed after 7 days. Regardless of the immersion time, the deposition of biomimetic calcium phosphate on the substrate generally depends on increasing the super-saturation degree of major apatite constructor ions and the presence of functional groups on the surface of the polymer inducing the heterogeneous nucleation [19]. Previous studies found that HAp was partially dissolved by pH decrease around the implants leading to the increased calcium, phosphate and hydroxyl ions and resulting in calcium deposition as the most basic step in apatite nucleation and growth process on the surface of implants [20]. This process was distinctly investigated in our research by rising HAp concentration from 1 to 3%, but it seemed that calcium phosphate nucleation and growth were slower in SF-5% HAp composites probably due to HAp nanoparticles agglomeration through increasing the percentages of these particles in SF.

The XRD results of nano fibres after 7 days immersion in Fig. 3*a* indicate two diffraction peaks 26.68° and 39.43° in SF-1%HAp. The peaks at 31.721° and 45.45° in SF-3%HAp were, respectively, ascribed to (002), (310), (211) and (222) planes of the precipitated HAp structure, and only a peak at 29.5° was probably corresponding to the formation of brushite crystals on SF-5%HAp nanofibres. The presence of transmittance peaks at 551, 699 and 1067 cm^{-1} in all of nanofibres in Fig. 3*b* and the strong carbonate group peak at

doi: 10.1049/mnl.2018.0047

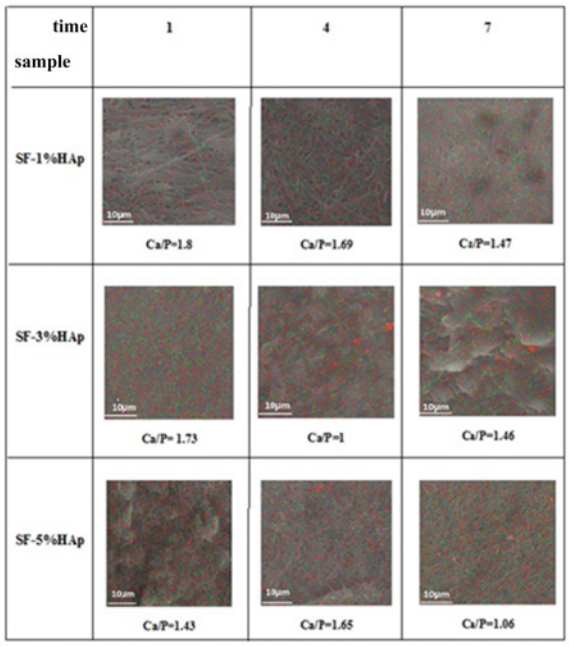

Fig. 2 *SEM/EDS analyses of SF-HAp nanofibres after 1, 4 and 7 days immersion in SBF*

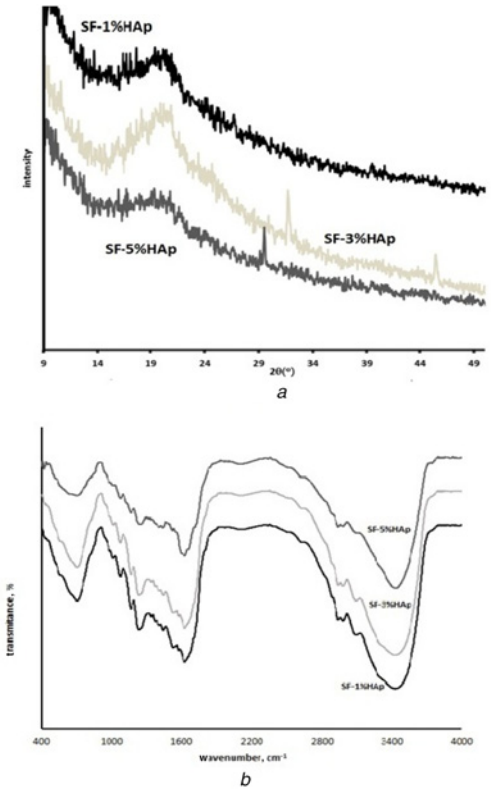

Fig. 3 *XRD patterns and FTIR spectra of SF-HAp nanofibres after 7-day immersion in SBF*
a XRD diffraction patterns
b FTIR spectra

1447 cm^{-1} again confirmed the formation of carbonate apatite on the surface of SF-HAp nano-composites [21].

3.4. Cellular assay

3.4.1. MTT assay: According to results of MTT in Fig. 4, the cell growth and proliferation were acceptable for nanofibres. In all

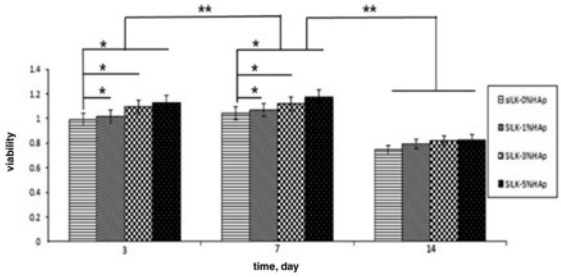

Fig. 4 *Viability of MG63 cells after exposed to nano fibres extracts* (** $p < 0.01$ and * $p < 0.05$)

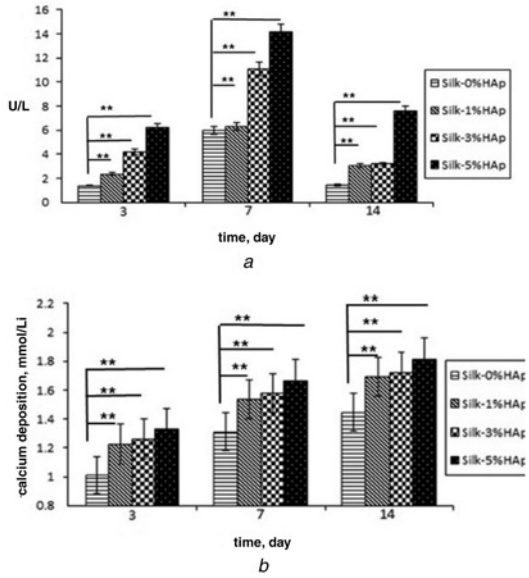

Fig. 5 *ALP activity and Calcium deposition analysis of MG63 cells in direct contact with SF-HAp nanofibres (** $p < 0.01$)*
a ALP activity
b Calcium deposition analysis

groups, the viability of MG-63 cells was significantly increased on day 7 compared to day 3 indicating the high cell metabolism. The biocompatibility of nano-composites significantly increased compared with the control group, and this upward trend was observed in all periods of time. These results reproved that HAp is a biocompatible material, and its composite with SF natural polymer could up-regulate the osteoblast metabolism [22]. On day 14, there was not any significant difference within the group; and a dramatic reduction was observed in the cell viability. This might be due to the enormous growth of cells following by the prevented contact [23].

3.4.2. ALP activity: Osteoblast cells participate in the bone formation process by ALP secretion and creation of alkaline environment [24]. Since this enzyme involves in the first step of bone mineralisation, the level of this enzyme secretion was measured on days 3, 7 and 14 (Fig. 5*a*). The obtained results indicated that the secreted enzyme was low on day 3, but reached its peak on day 7 indicating the osteogenic differentiation, while this activity significantly declined on day 14. In all periods of time, the SF/HAp composites attracted the osteoblast cells to the osteogenic differentiation, and thus the secretion of this enzyme was significantly higher than the SF nanofibres. The activities of this enzyme were probably increased by partial ceramic phase solution which increased the concentration of calcium ions in the culture medium [25]. Consistent with the previous studies, our results indicated

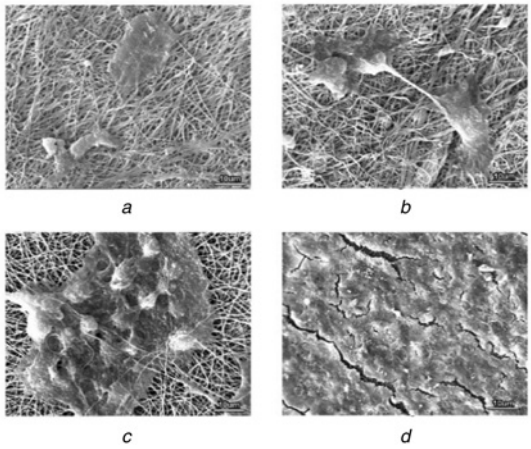

Fig. 6 *Cell adhesion of MG63 cells on the surface of SF-HAp nanofibres after 3 days*
a 0%
b 1%
c 3%
d 5% HAp content

that HAp, as an osteoconductive biomaterial, could accelerate the mineralisation process and enhance differentiation and gene expression of osteoblast cells [26].

3.4.3. Ca assay: The present research investigated the mineralisation as a fundamental indicator in osteogenic differentiation [27]. The calcium content considerably grew from days 3 to 14 in Fig. 5*b*. Within each group, the HAp nanoparticles increased the calcium deposition into SF nano-fibres. At any given time, this diagram peaked at 5% HAp samples, while there was a difference between SF-1%HAp and SF-3%HAp. According to ALP and Ca assay, it was found that the down regulation of ALP activity on day 14 after the highest activity on day 7 during osteogenic differentiation process coincided with higher mineralisation [28]. In general, the SF-5%HAp composites provided better conditions for the growth and proliferation of cells resulting in higher ALP activity and finally higher calcium deposition compared with other groups of nano-fibre.

3.4.4. Cell adhesion: According to Fig. 6, the SEM images indicated that the SF nanofibres and composites were biocompatible; and the osteoblast cells well adhered to the surface of nanofibres with cytoplasmic extension and bridging the porosities between the nanofibres. The number of attached cells is very low on the SF fibres, but the matrix provides a more suitable substrate for bone cell adhesion in SF-HAp mats. Meanwhile, the cell migration, adhesion and spreading were improved by increasing the HAp particles in matrix, so that the cell densities completely covered the surface of SF-5%HAp nanofibres. Improving the SF biocompatibility and increasing the hydrophilicity of SF nanofibres, the HAp nanoparticles create favourable conditions for osteoblast cells and this is consistent with results of the MTT assay [29].

4. Conclusion: The SF-HAp nano composites were synthesised by electrospinning in order to investigate the efficiency of distributed HAp nanoparticles on mechanical properties and cell compatibility of SF nano-fibres for bone tissue engineering. Different HAp nanoparticles were added to SF solution with the aim to achieve the uniform nano-composites. The results indicated that SF-3%HAp had both high tensile strength and toughness. In addition, all of the electrospun nano-composites had favourable osteoblast cell compatibility leading to the osteogenic differentiation of MG-63 cells and enhanced osteoblast cell adhesion by creating more suitable surface conditions than the SF nanofibres.

5. Acknowledgments: The authors are grateful to Iran National Science Foundation (grant no. 94811324) for the financial support of this project.

6 References

[1] Vepari C., Kaplan D.L.: 'Silk as a biomaterial', *Prog. Polym. Sci.*, 2007, **32**, pp. 991–1007
[2] Altman G.H., Diaz F., Jakuba C., *ET AL.*: 'Silk-based biomaterials', *Biomaterials*, 2003, **24**, pp. 401–416
[3] Kasoju N., Bora U.: 'Silk fibroin in tissue engineering', *Adv. Healthcare Mater.*, 2012, **1**, pp. 393–412
[4] Rajkhowa R., Gupta V.B., Kothari V.K.: 'Tensile stress–strain and recovery behavior of Indian silk fibers and their structural dependence', *Appl. Polym. Sci.*, 2000, **77**, pp. 2418–2429
[5] Ayutsede J., Gandhi M., Sukigara S., *ET AL.*: 'Regeneration of Bombyx mori silk by electrospinning. Part3: characterization of electrospun nonwoven mat', *Polymer*, 2005, **46**, pp. 1625–1634
[6] Bai L.Q., Zhu L.J., Min S.aJ., *ET AL.*: 'Surface modification and properties of *bombyx mori* silk fibroin films by antimicrobial peptide', *Appl. Surf. Sci.*, 2008, **254**, pp. 2988–2995
[7] Yucheng L., Yurong C., Xiangdong K., *ET AL.*: 'Anisotropic growth of hydroxyapatite on the silk fibroin films', *Appl. Surf. Sci.*, 2008, **255**, pp. 1681–1685
[8] Wei K., Li Y., Kim K.O., *ET AL.*: 'Fabrication of nano-hydroxyapatite on electrospun silk fibroin nanofiber and their effects in osteoblastic behavior', *Biomed. Mater. Res.*, 2011, **97**, (A), pp. 272–280
[9] Kim H.J., Kim U.-J., Kim H.S., *ET AL.*: 'Bone tissue engineering with premineralized silk scaffolds', *Bone*, 2008, **42**, pp. 1226–1234
[10] Sheikh F., Ju H.W., Moon B.M., *ET AL.*: 'A novel approach to fabricate silk nanofibers containing hydroxyapatite nanoparticles using a three-way stopcock connector', *Nanoscale Res. Lett.*, 2013, **8**, (1), pp. 303–317
[11] Kim H., Che L., Ha Y., *ET AL.*: 'Mechanically-reinforced electrospun composite silk fibroin nanofibers containing hydroxyapatite nanoparticles', *Mater. Sci. Eng. C*, 2014, **40**, pp. 324–335
[12] Ming J., Liu Z., Zhang F., *ET AL.*: 'Novel silk films prepared by formic acid/hydroxyapatite dissolution method', *Mater. Sci. Eng. C*, 2014, **37**, pp. 48–53
[13] Ming J., Zuo B.: 'A novel electrospun silk fibroin/hydroxyapatite hybrid nanofibers', *Mater. Chem. Phys.*, 2012, **137**, pp. 421–427
[14] Rockwood D.N., Preda R.C., Yücel T., *ET AL.*: 'Materials fabrication from Bombyx mori silk fibroin', *Nat. Protocols*, 2011, **6**, (10), pp. 1612–1631
[15] Hadisi Z., Nourmohammadi J., Haghighipour N., *ET AL.*: 'How direct electrospinning in methanol bath affects the physico-chemical and biological properties of silk fibroin nanofibrous scaffolds', *Micro Nano Lett.*, 2016, **11**, (9), pp. 514–517
[16] Mirahmadi F., Tafazzoli-Shadpour M., Shokrgozar M.A., *ET AL.*: 'Enhanced mechanical properties of thermosensitive chitosan hydrogel by silk fibers for cartilage tissue engineering', *Mater. Sci. Eng. C*, 2013, **33**, (8), pp. 4786–4794
[17] Ou Y., Yang F., Yu Z.-Z.: 'A new conception on the toughness of nylon6/silica nano composite prepared via in situ polymerization', *Polym. Sci. B Polym. Phys.*, 1998, **36**, pp. 789–795
[18] Wang M., Bonfield W.: 'Chemicaly coupled hydroxyapatite-polyethylene composites: structure and properties', *Biomaterials*, 2001, **22**, pp. 1311–1320
[19] Ethirajan A., Ziener U., Landfester K.: 'Surface-functionalized polymeric nanoparticles as templates for biomimetic mineralization of hydroxyapatite', *Chem. Mater.*, 2009, **21**, pp. 2218–2225
[20] von der Mark K., Park J.: 'Engineering biocompatible implant surfaces. Part II. Cellular recognition of biomaterial surfaces: lessons from cell–matrix interactions', *Prog. Mater. Sci.*, 2013, **58**, pp. 327–381
[21] Chang M., Douglas W., Tanaka J.: 'Organic- inorganic interaction and the growth mechanism of hydroxyapatite crystals in gelatin matrices between 37 and 80 C', *Mater. Sci. Mater. Med.*, 2006, **17**, pp. 387–396
[22] Jiang J., Hao W., Li Y., *ET AL.*: 'Hydroxyapatite/regenerated silk fibroin scaffold-enhanced osteoinductivity and osteoconductivity

doi: 10.1049/mnl.2018.0047

of bone marrow-derived mesenchymal stromal cells', *Biotechnol. Lett.*, 2013, **35**, pp. 657–661
[23] Zadegan S., Hossainalipour M., Ghassai H., *ET AL.*: 'Synthesis of cellulose–nanohydroxyapatite composite in 1-n-butyl-3-methylimidazolium chloride', *Ceram. Int.*, 2010, **36**, pp. 2375–2381
[24] Lao L., Wang Y., Zhu Y., *ET AL.*: 'Poly(lactide-co-glycolide)/hydroxyapatite nanofibrous scaffolds fabricated by electrospinning for bone tissue engineering', *Mater. Sci.: Mater. Med.*, 2011, **22**, pp. 1873–1884
[25] Zhang F., Zhang Z., Zhu X., *ET AL.*: 'Silk-functionalized titanium surfaces for enhancing osteoblast functions and reducing bacterial adhesion', *Biomaterials*, 2008, **29**, pp. 4751–4759
[26] Yu H., Hong S., Kim H.: 'Surface- mineralized polymeric nanofiber for the population and osteogenic stimulation of rat bone-marrow stromal cells', *Mater. Chem. Phys.*, 2009, **113**, pp. 873–880
[27] Narayanan R., Seshadri S.K., Kwon T.Y., *ET AL.*: 'Calcium phosphate-based coatings on titanium and its alloys', *Biomed. Mater. Res. Part B*, 2008, **85**, pp. 279–299
[28] Zhang X., Chang W., Lee P., *ET AL.*: 'Polymer-ceramic spiral structured scaffolds for bone tissue engineering: effect of hydroxyapatite composition on human fetal osteoblasts', *PLoS ONE*, 2014, **9**, (1), pp. 1–10
[29] Arima Y., Iwata H.: 'Effect of wettability and surface functional groups on protein adsorption and cell adhesion using well-defined mixed self-assembled monolayers', *Biomaterials*, 2007, **28**, pp. 3074–3082